

# ROSAT HRI observations of seven high redshift quasars

J. Siebert and W. Brinkmann

Max-Planck-Institut für extraterrestrische Physik, Giessenbachstrasse, D-85740 Garching, Germany

Received / Accepted

**Abstract.** We present ROSAT HRI observations of six quasars with redshifts  $\gtrsim 3.4$ : PKS 0335-122, S4 0620+389, B1422+231, PKS 2215+02, Q 2239-386 and PC 2331+0216. We include the observation of the radio-quiet quasar BG 57 9, whose redshift has recently been revised to  $z = 0.965$ . S4 0620+389, B1422+231, PKS 2215+02 and BG 57 9 are detected in the ROSAT energy band (0.1-2.4 keV).  $2\sigma$  upper limits are given for the remaining objects. All X-ray sources are point like to the limit of the HRI point spread function. We report marginal evidence for X-ray variability in S4 0620+389 on timescales of several hours (rest frame). No significant X-ray variability is found in the gravitationally lensed quasar B1422+231 on rest frame timescales of hours and months. We present the spectral energy distributions for six of the high redshift quasars and compare them to the mean distribution of low redshift quasars.

**Key words:** Galaxies: active – quasars: general – X-rays: galaxies

## 1. Introduction

The study of quasars at high redshifts is motivated by a number of interesting, yet unsolved questions: How (and when) have quasars formed? How do their spectral energy distributions change with time? What causes the differences between radio-loud and radio-quiet quasars and do these differences persist to high redshifts? The X-ray emission of quasars is particularly interesting, since it constitutes a large fraction of the bolometric luminosity of quasars (e.g. Elvis et al. 1994). Further, the X-rays are mostly produced in the innermost regions of the AGN and can therefore provide clues to our understanding of the 'central engine' and quasar evolution.

In the past, quasars with  $z > 3$  have mostly been studied in the optical and the radio band. Only the advent of missions like ROSAT (Trümper 1982) and ASCA (Tanaka et al. 1994), which combine high sensitivity with sufficient spatial and spectral resolution, has enabled the investigation of the X-ray properties of these high redshift objects. However, the number of

quasars with  $z > 3$ , which are detected in X-rays, is still low (e.g. Cappi et al. 1997). In order to draw statistically significant conclusions on the emission properties of high redshift quasars and possible differences to their local counterparts, it is clearly desirable to increase the number of sources with X-ray data.

We therefore observed with the ROSAT High Resolution Imager (HRI) four radio-loud (PKS 0335-122, S4 0620+389, B1422+231, PKS 2215+02) and two radio-quiet quasars (Q 2239-386, PC 2331+0216) at  $z > 3.4$ . The redshift of the radio-quiet quasar BG 57 9, originally cataloged with  $z = 3.74$  (Hewitt & Burbidge 1987), was recently revised to  $z = 0.965$  (Borra et al. 1996). Nevertheless, we present the X-ray observation in this paper. The basic properties of the observed quasars are summarized in Table 1. All quasars were previously not detected in X-rays. Due to its high spatial resolution and the achievable positional accuracy the HRI is very well suited to unambiguously identify the X-ray emission of high redshift quasars.

## 2. Observations and data reduction

The X-ray observations were performed with the ROSAT HRI between December 1994 and August 1996. Details of the individual observations are given in Table 2.

The data analysis was performed using standard routines within the EXSAS environment (Zimmermann et al. 1994). The count rates were determined with the standard maximum likelihood source detection algorithm, which delivers the source counts within 2.5 times the FWHM of the HRI point spread function. In case of no detection at the optical position of the quasar, i.e. if the respective likelihood was below 10, which corresponds to about  $4\sigma$ , we calculated the 90% upper limit for the count rate. The conversion to fluxes in the 0.1–2.4 keV energy band was done by assuming an average power law spectrum for the sources plus Galactic absorption (Dickey & Lockman 1990). Since no spectral information is available, the average power law index for high redshift quasars was adopted ( $\Gamma \sim 1.7$  and  $\Gamma \sim 2.0$  for radio-loud and radio-quiet quasars, respectively [Brinkmann, Yuan & Siebert 1997; Yuan et al. 1998]). Finally, luminosities were computed assuming  $H_0 = 50 \text{ km s}^{-1} \text{ Mpc}^{-1}$ ,  $q_0 = 0.5$  and isotropic emission.

**Table 1.** Properties of the observed high redshift quasars.

Name	Position (J2000.0)	$z$	Ref.	$m$	Ref.	$f_{5\text{ GHz}}$
(1)	(2)	(3)	(4)	(5)	(6)	(7)
PKS 0335-122	03 37 55.7 -12 04 12.0	3.442	O94	r19.79	C85	293±19 mJy
S4 0620+389	06 24 19.0 +38 56 48.7	3.469	X94	r20.0	SK96	836±74 mJy
B1422+231	14 24 38.1 +22 56 00.1	3.62	P92	v16.71	R93	548±49 mJy
PKS 2215+02	22 17 48.3 +02 20 12.1	3.581	S90	b21.97	D97	513±46 mJy
BG 57 9	13 07 02.7 +29 18 42.3	3.74	V82	v20.14	B90	...
	...	0.965	B96	...	...	...
Q 2239-386	22 41 51.8 -38 20 17.2 <sup>†</sup>	3.511	ST90	...	...	...
PC 2331+0216	23 34 32.0 +02 33 21.8	4.093	S94	r19.98	S89	3.3 mJy <sup>‡</sup>

<sup>†</sup> Uncertainty of the position  $\sim 150'' \times 150''$

<sup>‡</sup> Radio flux from Schneider et al. (1992)

(1) Common name; (2) Optical position (J2000.0); (3) Redshift; (4) Reference for the redshift: Borra et al. 1996 (B96), Osmer et al. 1994 (O94), Patnaik et al. 1992 (P92), Savage et al. 1990 (S90), Schneider et al. 1994 (S94), Steidel 1990 (ST90), Vaucher 1982 (V82), Xu et al. 1995 (X94); (5) Optical magnitude. The letter indicates the observing band:  $b = B_J$  ( $\approx 4680\text{\AA}$ ),  $v = \text{Johnston V}$  ( $\approx 5500\text{\AA}$ ),  $r = \text{Gunn r}$  ( $\approx 6500\text{\AA}$ ); (6) Reference for the optical magnitude: Beauchemin et al. 1990 (B90), Chu et al. 1985 (C85), Drinkwater et al. 1997 (D97), Remy et al. 1993 (R93), Schneider et al. 1989 (S89), Stickel & Kühr 1996 (SK96); (7) Total 5 GHz radio flux density from the GB6 radio catalog (Gregory et al. 1996).

The results of the analysis and the derived X-ray properties are summarized in Table 2.

### 3. Notes on individual sources

#### 3.1. PKS 0335-122, $z = 3.442$

This is an optically faint radio-loud quasar with a Gunn  $r$  ( $\approx 6500\text{\AA}$ ) magnitude of 19.79 (Chu et al. 1985). On the digitized POSS plates a stellar object with  $m_B = 21.44$  is found. The radio spectrum is flat ( $\alpha_{2.7}^5 \approx 0.08$ ,  $S_\nu \propto \nu^\alpha$ ; Véron-Cetty & Véron 1993, VV93 hereafter). The 5 GHz radio emission is clearly variable, since the radio flux density is  $293 \pm 19$  mJy according to the PMN catalog (Griffith & White 1993), whereas the higher resolution NVSS (Condon et al. 1997) gives  $475.7 \pm 14.3$  mJy.

The exposure of PKS 0335-122 was only  $\sim 1400$  seconds and the source was not detected in this observation. The resulting  $2\sigma$  upper limits are  $7.3 \times 10^{-14}$  erg cm $^{-2}$  s $^{-1}$  and  $7.8 \times 10^{45}$  erg s $^{-1}$  for the (unabsorbed) 0.1–2.4 keV flux and luminosity, respectively. We can roughly estimate the expected X-ray luminosity by using the known correlation with total radio luminosity, e.g.  $\log L_{0.1-2.4\text{keV}} = 0.7 \log L_{\text{total},5\text{GHz}} + 21.3$  (Brinkmann et al. 1997). It turns out that the upper limit is almost a factor of two higher than the estimated X-ray luminosity of  $\sim 4 \times 10^{45}$  erg s $^{-1}$ .

#### 3.2. S4 0620+389, $z = 3.469$

Optically faint ( $m_R = 20.0$ ), but radio bright quasar. The total 5 GHz flux density is  $836 \pm 74$  mJy (Gregory et al. 1996). In the NVSS it had  $808.6 \pm 24.3$  mJy. S4 0620+389 has been the target

of various VLBI observations (e.g. Morabito et al. 1986; Xu et al. 1995). The radio source was not resolved and it displayed a 5 GHz VLBI flux density of 436 mJy (Xu et al. 1995). A comparatively high degree of polarization of the radio emission has been reported ( $P \sim 4\%$ ; Okudaira et al. 1993).

S4 0620+389 is a fairly strong X-ray source with an unabsorbed 0.1–2.4 keV flux of  $5.8 \times 10^{-13}$  erg cm $^{-2}$  s $^{-1}$  and a corresponding luminosity of  $3.5 \times 10^{46}$  erg s $^{-1}$  in the HRI observation. In view of this relatively high X-ray flux, we analyzed the latest reprocessing of the ROSAT All-Sky Survey (RASS) data for this source. We find an X-ray source at the position of S4 0620+389 with  $\sim 3.5\sigma$  significance. The count rate is  $0.023 \pm 0.009$ , which corresponds to  $(7.5 \pm 2.9) \times 10^{-13}$  erg cm $^{-2}$  s $^{-1}$ . The RASS flux is thus fully consistent with the HRI flux.

We compared the radial profile of S4 0620+389 with the properly normalized intensity profile of the BL Lac object PKS 2155-304 and found no evidence for extended emission to the limit of the point spread function of the HRI (FWHM  $\sim 5''$ ), which corresponds to about 34 kpc in the rest frame of S4 0620+389 assuming  $H_0 = 50$  km s $^{-1}$  Mpc $^{-1}$  and  $q_0 = 0.5$ .

S4 0620+389 is bright enough to check for variability within the observation. We divided the total observation into four contiguous observation intervals, one on each day between April, 5 and April, 8 1996, with individual exposures ranging from 2.2 to 7.8 ksec. We then applied a maximum-likelihood source detection on each of these intervals separately. The resulting count rates are shown in Fig. 1 as a function of time. There is evidence for X-ray variability by a factor of two on a timescale of  $\sim 1.5$  days ( $\sim 8$  hours rest frame), however, only

**Table 2.** ROSAT observation log and results.

Name	Obs. date	Exp. [s]	cts/s [ $10^{-3} \text{ s}^{-1}$ ]	$N_{\text{H}}$ [ $\text{cm}^{-2}$ ]	$f_{\text{x}}$ [ $\text{erg cm}^{-2} \text{ s}^{-1}$ ]	$L_{\text{x}}$ [ $\text{erg s}^{-1}$ ]
(1)	(2)	(3)	(4)	(5)	(6)	(7)
PKS 0335-122	08/27 - 08/28/96	1423	<1.26	4.08	$< 7.3 \times 10^{-14}$	$< 7.8 \times 10^{45}$
S4 0620+389	04/05 - 04/08/96	17808	$6.53 \pm 0.64$	17.10	$(5.8 \pm 0.6) \times 10^{-13}$	$3.5 \times 10^{46}$
B1422+231a	01/27/95	5678	$14.98 \pm 1.67$	2.49	$(7.7 \pm 0.9) \times 10^{-13}$	$5.1 \times 10^{46}$
B1422+231b	01/18 - 01/26/96	10918	$12.43 \pm 1.10$	2.49	$(6.4 \pm 0.6) \times 10^{-13}$	$4.2 \times 10^{46}$
PKS 2215+02	05/29 - 06/05/95	14671	$5.40 \pm 0.64$	4.76	$(3.2 \pm 0.4) \times 10^{-13}$	$2.1 \times 10^{46}$
BG 57 9	07/10 - 07/13/95	10630	$0.93 \pm 0.34$	2.97	$(5.0 \pm 1.8) \times 10^{-14}$	$2.7 \times 10^{44\dagger}$
Q 2239-386	05/24 - 05/25/95	17094	<0.38	4.69	$< 2.3 \times 10^{-14}$	$< 2.3 \times 10^{45}$
PC 2331+0216	12/24 - 12/26/94	15771	<0.62	1.18	$< 2.7 \times 10^{-14}$	$< 3.8 \times 10^{45}$

† Assuming  $z = 3.74$ :  $L_{\text{x}} = 5.7 \times 10^{45} \text{ erg s}^{-1}$

(1) Common name; (2) Date of the HRI observation; (3) Effective, vignetting and dead time corrected exposure in seconds; (4) Count rate or  $2\sigma$  upper limit; (5) Galactic  $N_{\text{H}}$  from Dickey & Lockman (1990) and Stark et al. (1992); (6) unabsorbed 0.1–2.4 keV flux; (7) 0.1–2.4 keV luminosity assuming  $H_0 = 50 \text{ km s}^{-1} \text{ Mpc}^{-1}$  and  $q_0 = 0.5$ .

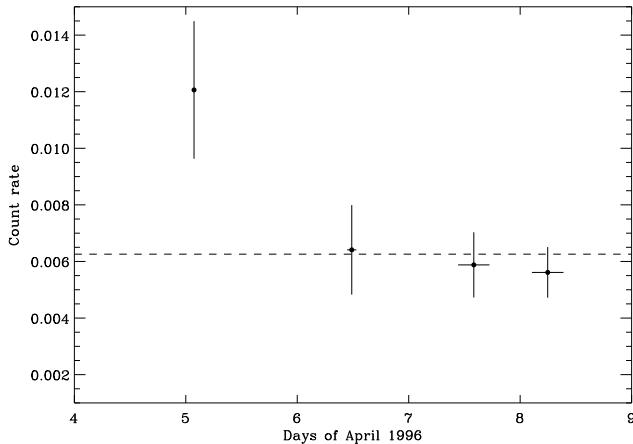


**Fig. 1.** X-ray light curve of S4 0620+389. The horizontal error bars indicate the length of the individual observation interval. The dotted line denotes the weighted average of the count rate.

with marginal significance. The highest and the lowest count rate differ by  $\sim 2\sigma$ .

### 3.3. BG 57 9 ([HB89] 1304+295), $z = 0.965$

In the Hewitt & Burbidge (1987; HB87 hereafter) catalog a redshift of  $z = 3.74$  is given for this source. This value was originally determined by Vaucher (1982). Recently, Borra et al. (1996) presented new optical data and they report a redshift of  $z = 0.965$ . Although BG 57 9 might therefore not qualify anymore for our high redshift sample, we still present its X-ray properties in this paper. The best upper limit on the radio emission is  $f_{1.4\text{GHz}} < 2.5 \text{ mJy}$ , which corresponds to the

sensitivity limit of the NVSS. Using  $m_{\text{v}} = 20.14$ ,  $f_{1.4\text{GHz}} = 2.5 \text{ mJy}$  and  $\alpha_{\text{opt}} = \alpha_{\text{r}} = 0.5$  the K-corrected ratio  $R = \log(f_{5\text{GHz}}/f_{4400\text{\AA}})$  is  $\sim 1.5$ . This is slightly above the commonly accepted dividing line between radio-loud and radio-quiet quasars ( $R = 1$ ; Kellerman et al. 1989). With present data it therefore cannot be excluded that BG 57 9 is a radio-loud quasar.

The source is marginally detected in our 10.6 ksec HRI observation. The detection likelihood is 10.6, which corresponds to about  $4.3\sigma$ . The positional difference between the X-ray and the optical position is only  $0.8''$ . We are therefore confident that the detected X-ray source is associated with the quasar. The 0.1–2.4 keV flux of the source is  $5.0 \times 10^{-14} \text{ erg cm}^{-2} \text{ s}^{-1}$ . Applying the new redshift of BG 57 9, this gives a luminosity of  $2.7 \times 10^{44} \text{ erg s}^{-1}$ .

### 3.4. B1422+231, $z = 3.62$

This object is a optically and radio bright, gravitationally lensed quasar at a redshift of  $z = 3.62$ . The original radio map shows four components within  $1.3''$  (Patnaik et al. 1992). Subsequent optical and infrared observations confirmed the lensing hypothesis and discovered variability in the three brightest components (Lawrence et al. 1992; Yee & Bechtold 1996). A recent HST observation revealed the lensing galaxy at a redshift of  $z \sim 0.4$  close to the faintest quasar image (Impey et al. 1996).

B1422+231 was observed twice with the HRI: for  $\sim 5.7$  ksec in January 1996 and for another  $\sim 10.9$  ksec about one year later. It is clearly detected in both observations and the 0.1–2.4 fluxes are  $(7.7 \pm 0.9) \times 10^{-13} \text{ erg cm}^{-2} \text{ s}^{-1}$  and  $(6.4 \pm 0.6) \times 10^{-13} \text{ erg cm}^{-2} \text{ s}^{-1}$ , respectively. The X-ray emission has not varied significantly between the two observa-

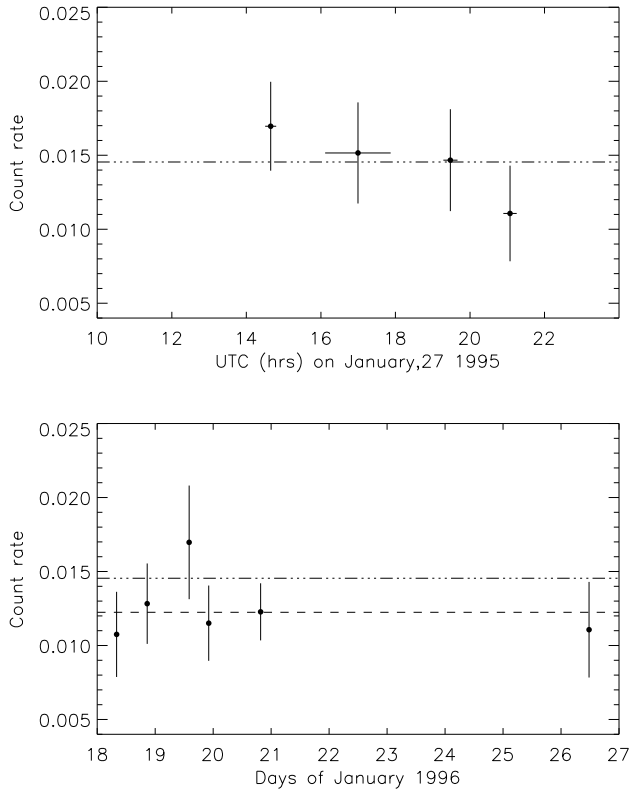


**Fig. 2.** X-ray light curve of the gravitationally lensed system B1422+231. The dash-dotted and the dashed line denote the weighted averages of the count rates in the first (top panel) and the second observation (bottom panel), respectively.

tions. Analyzing the reprocessed ROSAT All-Sky Survey data, we find that B1422+231 is marginally detected ( $3.7\sigma$ ). The X-ray flux in the Survey is  $(4.5 \pm 1.2) \times 10^{-13} \text{ erg cm}^{-2} \text{ s}^{-1}$ , which might indicate that B1422+231 has varied in X-rays between the All-Sky Survey and the HRI observation ( $\Delta T \sim 5$  years, i.e.  $\sim 1$  year rest frame).

Next we looked for X-ray variability within each of the two observations of B1422+231. We divided the observations into several contiguous intervals with individual exposures between 1.2 and 2 ksec and applied a maximum-likelihood source detection on each of the intervals separately. The resulting count rates are shown in Fig. 2 as a function of time. Although the light curve suggests some trends in the count rate, a  $\chi^2$  test gives no indication for significant variability ( $\chi^2_\nu = 0.58$  (9 dof)).

The X-ray surface brightness profile for B1422+231 is shown in Fig. 3 in comparison to that of a  $\sim 50$  ksec HRI observation of the BL Lac object PKS 2155-304. The profile of PKS 2155-304 was normalized to the first bin of the radial profile of B1422+231. The local background intensity was determined from an annulus with inner radius  $2.5'$  and outer radius  $5'$  around B1422+231 and then added to the intensity profile of PKS 2155-304. There is no evidence for sig-

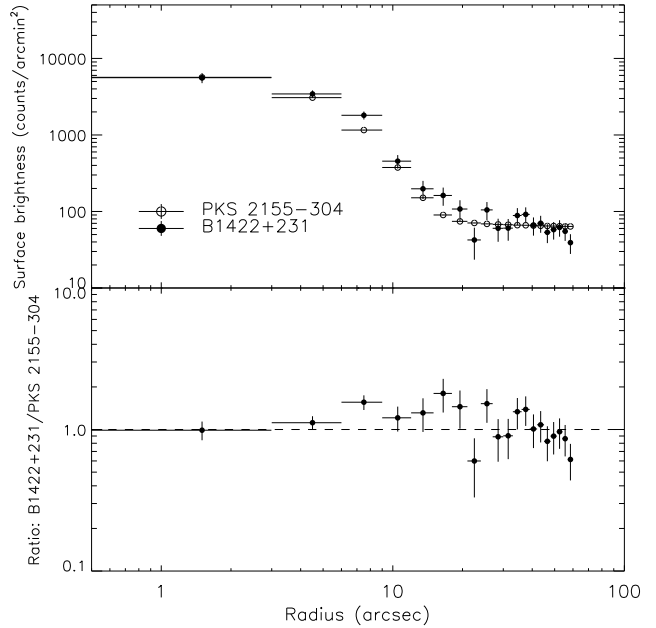


**Fig. 3.** The radial X-ray surface brightness profile of B1422+231 compared to that of the BL Lac object PKS 2155-304. The latter has been normalized to the first bin of the B1422+231 profile. The bottom panel shows the ratio of the two intensity profiles. No significantly extended X-ray emission is found.

nificantly extended X-ray emission to the limit of the PSF of the ROSAT HRI (FWHM  $\sim 5''$ , which corresponds to about 34 kpc for  $z = 3.62$ ). The systematic trend, which is visible in the lower panel of Fig. 3 up to a radius of  $20''$ , is most likely due to the energy dependent PSF of the HRI, which is slightly more extended for higher energies. Since the average soft X-ray spectrum of high redshift radio-loud quasars is much harder ( $\Gamma \approx 1.7$ ; e.g. Siebert et al. 1996) than that of PKS 2155-304 ( $\Gamma \approx 2.65$ ; Brinkmann et al. 1994), the radial profile of B1422+231 appears to be slightly extended.

### 3.5. PKS 2215+02, $z = 3.581$

Optically very faint ( $m_B = 21.97$ ) radio-loud quasar at a redshift of  $z = 3.581$ . The radio spectrum of PKS 2215+02 between 2.7 GHz and 5 GHz is flat ( $\alpha = -0.05$ , VV93) and the source seems to be variable in the radio band, since the flux density from the 87GB survey ( $f_{5 \text{ GHz}} = 513 \pm 46 \text{ mJy}$ ; Gregory et al. 1996) is significantly lower than the flux density measured four years later in the PMN survey ( $f_{5 \text{ GHz}} = 642 \pm 35 \text{ mJy}$ ; Griffith & White 1993) with an angular resolution comparable to the 87GB survey.

The source was clearly detected in our 14.7 ksec HRI observation. The X-ray position from the maximum-likelihood algorithm and the best known optical position of PKS 2215+02 differ by  $4.5''$ . This difference is easily explained by the ex-

pected residual boresight errors (e.g. Voges 1992). The unabsorbed 0.1–2.4 keV flux is  $3.2 \times 10^{-13} \text{ erg cm}^{-2} \text{ s}^{-1}$ , which gives an X-ray luminosity in the ROSAT band of  $2.1 \times 10^{46} \text{ erg s}^{-1}$ . The radial profile is consistent with the point spread function of the HRI, therefore no evidence for extended X-ray emission is found.

No source is detected in the RASS and the  $2\sigma$  upper limit ( $6.4 \times 10^{-13} \text{ erg cm}^{-2} \text{ s}^{-1}$ ) is well above the actual X-ray flux measured with the HRI.

### 3.6. Q 2239-386, $z = 3.511$

The position of this quasar is only poorly known and the positions given in VV93 and Hewitt & Burbidge (1993; HB93) are inconsistent. We adopt the position given in HB93 in this paper. The positional uncertainty listed in HB93 is of the order of  $\sim 150''$ . To our knowledge, no optical magnitude for this quasar is reported in the literature. Due to the poorly constrained optical position, the search for an optical counterpart on digitized POSS plates is not feasible (there are about 50 objects within  $150''$  of the given optical position). Imaging spectroscopy of this field is clearly warranted.

The upper limit to the X-ray flux at the position given in HB93 is  $2.3 \times 10^{-14} \text{ erg cm}^{-2} \text{ s}^{-1}$ , which corresponds to  $L_{0.1-2.4\text{keV}} = 2.3 \times 10^{45} \text{ erg s}^{-1}$ .

We note that there is an X-ray source at a distance of  $\sim 3'$  from the position of HB93 with a 0.1–2.4 keV flux of  $\sim 2 \times 10^{-13} \text{ erg cm}^{-2} \text{ s}^{-1}$ . In the vicinity of this X-ray source two objects can be found on the digitized POSS plate: a 14.78 mag stellar object at a distance of  $3.3''$  and a 18.39 mag galaxy at a distance of  $9.1''$  from the X-ray position. Both possible identifications suggest that this X-ray source is not associated with the high redshift quasar.

### 3.7. PC 2331+0216, $z = 4.093$

This quasar, originally classified as radio-quiet, has the highest redshift of the present sample. Schneider et al. (1992) report a 5 GHz flux density of 3.3 mJy. Using  $m_r = 19.98$ , we get  $R \approx 1.8$  for the K-corrected logarithmic ratio of 5 GHz radio to 4400Å optical flux. Therefore PC 2331+0216 is at the borderline between radio-loud and radio-quiet quasars.

PC 2331+0216 was not detected in our  $\sim 16$  ksec observation with the HRI. The  $2\sigma$  upper limit to the 0.1–2.4 keV flux is  $2.7 \times 10^{-14} \text{ erg cm}^{-2} \text{ s}^{-1}$ , which leads to a luminosity upper limit of  $3.8 \times 10^{45} \text{ erg s}^{-1}$ .

## 4. Spectral energy distributions

In Fig. 4 we present the spectral energy distributions (SED) from radio to X-ray frequencies for six of the high redshift quasars. Q 2239-386 is omitted from this analysis. All fluxes are given in the rest frame of the sources. Radio fluxes at various frequencies are used as listed in NED. In the case of BG 57 9 we also used the upper limit from the NVSS (Condon et al. 1997). Optical fluxes are calculated from the magnitudes given

in Table 1 and corrected for Galactic reddening as follows (e.g. Zombeck 1990):

$$f_{6500} = 10^{-0.4 \cdot (m_r - A_r) - 19.547} \text{ erg cm}^{-2} \text{ s}^{-1} \text{ Hz}^{-1}$$

$$f_{5500} = 10^{-0.4 \cdot (m_v - A_v) - 19.435} \text{ erg cm}^{-2} \text{ s}^{-1} \text{ Hz}^{-1}$$

$$f_{4400} = 10^{-0.4 \cdot (m_b - A_b) - 19.369} \text{ erg cm}^{-2} \text{ s}^{-1} \text{ Hz}^{-1}$$

The Galactic extinction at various wavelengths has been calculated from  $A_B$  as given in NED by using the reddening law from Seaton et al. (1979). In the case of B1422+231 we added a data point in the UV from the IUE observation ( $f_\lambda \approx 1.1 \times 10^{-15} \text{ erg s}^{-1} \text{ cm}^{-2} \text{ \AA}^{-1}$  between 1250 and 2000 Å) and in the near-infrared from Lawrence et al. (1992), who give an upper limit to the K-band ( $2.2\mu\text{m}$ ) emission of 12.7 mag. This magnitude was converted to a flux according to the formula (e.g. Wamsteker et al. 1981):

$$f_{2.2} = 10^{-0.4 \cdot m_K - 20.172} \text{ erg cm}^{-2} \text{ s}^{-1} \text{ Hz}^{-1}$$

The monochromatic X-ray fluxes (and upper limits) at 1 keV were calculated assuming  $\Gamma = 1.7$  for radio-loud and  $\Gamma = 2$  for radio-quiet quasars. All fluxes were finally transformed to the rest frame of the source.

For comparison we plot in Fig. 4 the mean SED of radio-loud (dotted) and radio-quiet (dashed) quasars as given in Elvis et al. (1994). The SEDs are arbitrarily normalized to the X-ray fluxes. Since the Elvis et al. (1994) sample contains X-ray bright *Einstein* IPC detected quasars, the mean SED tends to fall below the observed quasars at optical and radio wavelengths when it is normalized to the X-ray flux.

Taking this into account, most of the high redshift SEDs agree reasonably well with the low redshift mean. The systematically higher radio emission is a general feature of the SEDs of high redshift radio-loud quasars (Bechtold et al. 1994; Siebert et al. 1996). Still, remarkable differences between the radio-loud quasars are obvious from Fig. 4 with the two extremes being B1422+231 and PKS 2215+02. The main difference appears in the optical, where PKS 2215+02 is about two orders of magnitude fainter than B1422+231, whereas the X-ray and the radio fluxes are roughly comparable. This result might be explained by significant dust extinction intrinsic to the source. We note, however, that Francis et al. (in prep.) give an optical slope of  $\alpha_{\text{opt}} \approx -1$  for PKS 2215+02, which does not indicate a particularly red continuum compared to the other flat-spectrum quasars of their sample.

The SED of PC 2331+0216 fits remarkably well to the mean SED of low redshift radio-loud quasars. In particular the radio flux is almost three orders of magnitude higher than expected for an average radio-quiet quasar. Therefore PC 2331+0216 should indeed be considered as a radio-loud quasar.

In Table 3 we list the two-point spectral indices  $\alpha_{\text{ox}}$ ,  $\alpha_{\text{ro}}$  and  $\alpha_{\text{rx}}$  between the radio (4.85 GHz), the UV/optical (2500 Å) and the X-ray band (2 keV). The spectral indices are defined as follows:

$$\alpha_{\text{ox}} = 0.384 \times \log(f_o/f_x)$$

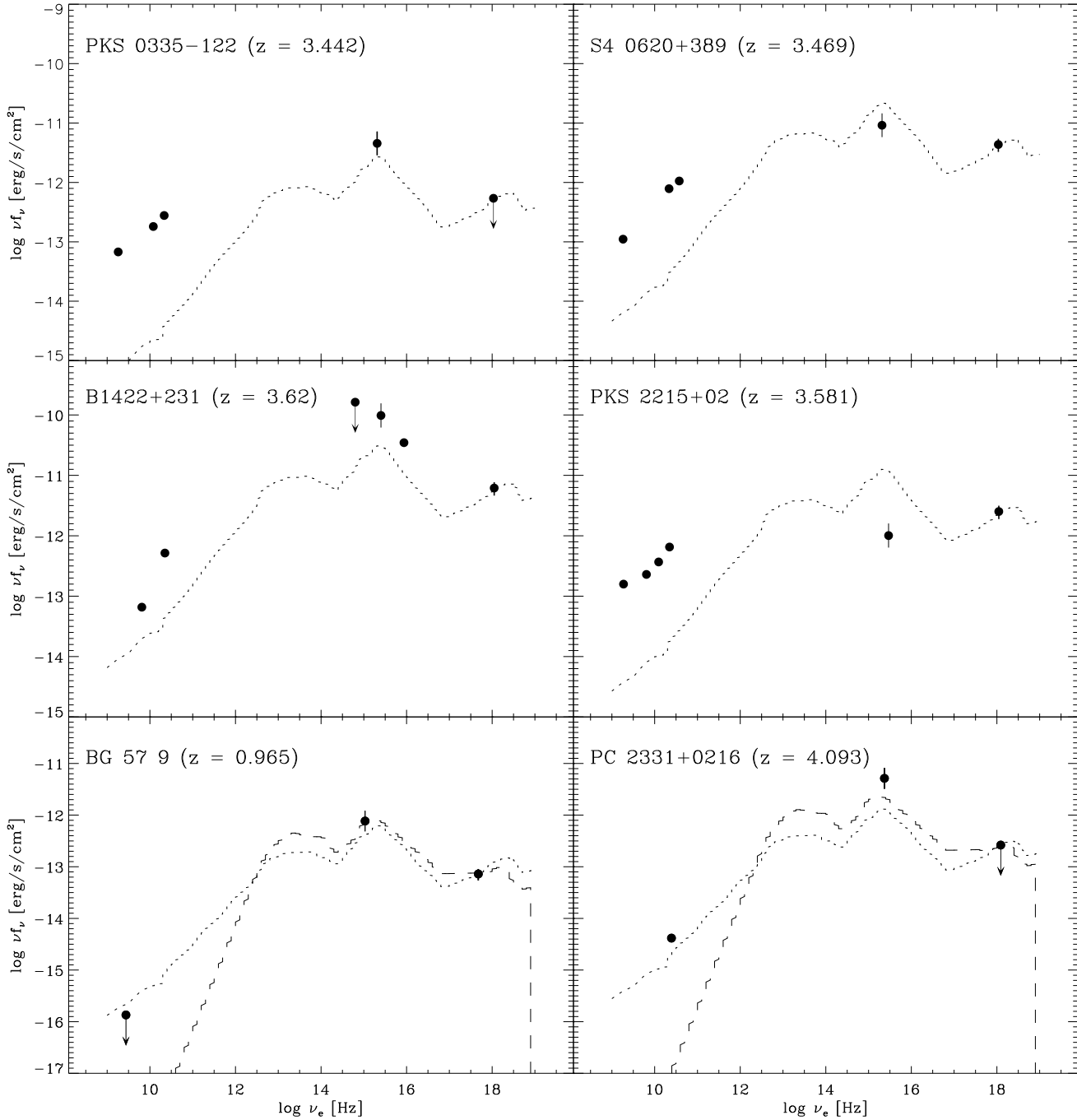


**Fig. 4.** The spectral energy distribution for the four radio-loud quasars (upper four panels) and two of the radio-quiet quasars. The dotted and the dashed lines represent the mean spectral energy distribution of radio-loud and radio-quiet quasars, respectively, as given in Elvis et al. (1994). The spectral energy distributions are arbitrarily normalized to the 1 keV flux.

$$\alpha_{\text{ro}} = 0.185 \times \log(f_{\text{r}}/f_{\text{o}})$$

$$\alpha_{\text{rx}} = 0.125 \times \log(f_{\text{r}}/f_{\text{x}})$$

where  $f_{\text{x}}$ ,  $f_{\text{o}}$  and  $f_{\text{r}}$  are the rest frame fluxes at the three frequencies given above.

$\alpha_{\text{ox}}$  and  $\alpha_{\text{ro}}$  both show a large scatter for the radio-loud quasars and the corresponding flux/luminosity ratios vary by factors of 40 to 80. This scatter is obviously mostly due to the optical emission, because the radio-to-X-ray spectral index  $\alpha_{\text{rx}}$  is almost constant for all four objects. The  $\alpha_{\text{ox}}$  values are

**Table 3.** Two point spectral indices.

Name	$\alpha_{\text{ox}}$	$\alpha_{\text{ro}}$	$\alpha_{\text{rx}}$
PKS 0335-122	>1.38	0.70	>0.92
S4 0620+389	1.14	0.73	0.86
B1422+231	1.50	0.50	0.82
PKS 2215+02	0.90	0.85	0.87
BG 57 9	1.42	<0.35	<0.70
PC 2331+0216	>1.42	0.34	>0.70

roughly consistent with the previously found mean values for larger samples. Brinkmann et al. (1997) give  $\langle\alpha_{\text{ox}}\rangle = 1.24$  for a sample of 297 flat-spectrum radio-loud quasars and Bechtold et al. (1994) find  $\alpha_{\text{ox}} \sim 1.4$  for high redshift quasars. As already noted, PKS 2215+02 is underluminous in the optical, which results in a very flat  $\alpha_{\text{ox}}$  of 0.9. There is only one high redshift quasar known, which exhibits a similarly extreme optical-to-X-ray ratio, namely 1745+624 ( $\alpha_{\text{ox}} \approx 0.8$ ; Fink & Briel 1993).

## 5. Summary

We presented ROSAT HRI observations of six quasars with redshifts  $z \gtrsim 3.4$  and one with  $z = 0.965$ . Four objects (S4 0620+389, B1422+231, PKS 2215+02, BG 57 9) are detected with X-ray luminosities ranging from  $2.7 \times 10^{44} \text{ erg s}^{-1}$  to  $5.1 \times 10^{46} \text{ erg s}^{-1}$ .  $2\sigma$  upper limits are given for the remaining three objects (PKS 0335-122, Q 2239-386, PC 2331+0216).

All X-ray sources are point like to the limit of the ROSAT HRI point spread function ( $\approx 5''$ , which corresponds to about 34 kpc at  $z = 3.5$ ).

We find marginal evidence for X-ray variability by a factor of two within the observation of S4 0620+389, i.e. on a timescale of several hours in the rest frame of the source. The gravitationally lensed system B1422+231 shows no indication for X-ray variability during the individual observations as well as between the two HRI observations, which are separated by about one year.

The spectral energy distributions of six of the high redshift quasars are presented. Although they are roughly consistent with the mean SED of low redshift quasars (Elvis et al. 1994), pronounced differences between individual objects appear. In particular PKS 2215+02 is almost two orders of magnitudes fainter in the optical compared to B1422+231, while the radio and the X-ray luminosities differ by only a factor of two. However, the optical continuum slope measured by Francis et al. (in prep.) does not indicate significant extinction by dust.

*Acknowledgements.* This research has made use of the NASA/IPAC Extragalactic Data Base (NED) which is operated by the Jet Propulsion Laboratory, California Institute of Technology, under contract with the National Aeronautics and Space Administration.

## References

Beauchemin M., Borra E.F., Edwards G., 1990, MNRAS 247, 182

- Bechtold J., Elvis M., Fiore F., et al., 1994, AJ 108, 374  
 Borra E.F., Levesque S., Beauchemin M., et al., 1996, AJ 111, 1456  
 Brinkmann W., Maraschi L., Treves A., et al., 1994, A&A 288, 433  
 Brinkmann W., Yuan W., Siebert J., 1997, A&A 319, 413  
 Cappi M., Matsuoka M., Comastri A., et al., 1997, ApJ 478, 492  
 Chu Y.Q., Zhu X.F., Butcher H., 1985, Chin. Astron. Astrophys. 9, 246  
 Condon J.J., Cotton W.D., Greisen E.W., 1997, <http://www.cv.nrao.edu/jcondon/mvss.html>  
 Dickey J.M., Lockman F.J., 1990, ARA&A 28, 215  
 Drinkwater M.J., Webster R.L., Francis P.J., et al., 1997, MNRAS 284, 85  
 Elvis M., Wilkes B.J., McDowell J.C., et al., 1994, ApJS 95, 1  
 Fink H.H., Briel U.G., 1993, A&A 274, L45  
 Gregory P.C., Scott W.K., Douglas K., Condon J.J., 1996, ApJS 103, 427  
 Griffith M.R., White A.E., 1993, AJ 105, 1666  
 Hewitt A., Burbidge G., 1987, ApJS 63, 1  
 Hewitt A., Burbidge G., 1993, ApJS 87, 451  
 Impey C.D., Foltz C.B., Petry C.E., Browne I.W.A., Patnaik A.R., 1996, ApJ 462, L53  
 Kellerman K.I., Sramek R., Schmidt M., Shaffer D. B., Green R., 1989, AJ 98, 1195  
 Morabito D.D., Niell A.E., Preston R.A., et al., 1986, AJ 91, 1038  
 Lawrence C.R., Neugebauer G., Weir N., Matthews K., Patnaik A.R., 1992, MNRAS 259, 5p  
 Okudaira A., Tabara H., Kato T., Inoue M., 1993, PASJ 45, 153  
 Osmer P.S., Porter A.C., Green R.F., 1994, ApJ 436, 678  
 Patnaik A.R., Browne I.W.A., Walsh D., Chaffee F.H., Foltz C.B., 1992, MNRAS 259, 1p  
 Remy M., Surdej J., Smette A., Claeskens J.F., 1993, A&A 278, L19  
 Savage A., Jauncey D.L., White G.L., et al., 1990, Aust. J. Phys. 43, 241  
 Schneider D.P., Schmidt M., Gunn J.E., 1989, AJ 98, 1507  
 Schneider D.P., van Gorkum J.H., Schmidt M., Gunn J.E., 1992, AJ 103, 1451  
 Schneider D.P., Schmidt M., Gunn J.E., 1994, AJ 107, 1245  
 Seaton M.J., 1979, MNRAS 187, 73p  
 Siebert J., Matsuoka M., Brinkmann W., et al., 1996, A&A 307, 8  
 Stark A.A., Gammie C.F., Wilson R.W., et al., 1992, ApJS 79, 77  
 Steidel C.C., 1990, ApJS 72, 1  
 Stickel M., Kühr H., 1996, A&AS 115, 11  
 Tanaka Y., Inoue H., Holt S.S., 1994, PASJ 46, L37  
 Trümper J., 1982, Adv. Space Res. 2, 241  
 Vaucher B.G., 1982, PhD thesis, Penn State University  
 Véron-Cetty M.-P., Véron P., 1993, A Catalogue of Quasars and Active Nuclei (6th edition), ESO Scientific Report No. 13  
 Voges W., 1992, in: Proceedings of the ISY conference "Space Science", ESA ISY-3, ESA Publications, p. 223  
 Wamsteker W., 1981, A&A 97, 329  
 Xu W., Readhead A.C.S., Pearson T.J., Polatidis A.G., Wilkinson P.N., 1995, ApJS 99, 297  
 Yuan W., Brinkmann W., Siebert J., 1998, A&A 330, 108  
 Yee H.K.C., Bechtold J., 1996, AJ 111, 1007  
 Zimmermann H.U., Becker W., Belloni T., et al., 1994, EXSAS User's Guide, MPE Report 257  
 Zombeck M.V., Handbook of Space Astronomy and Astrophysics, Cambridge University Press, Cambridge, p. 100